NANO LETTERS

2007
Vol. 7, No. 5
1318−1322

Immuno Gold Nanocages with Tailored Optical Properties for Targeted Photothermal Destruction of Cancer Cells

Jingyi Chen,[†] Danling Wang,[‡] Jiefeng Xi,[‡] Leslie Au,[†] Andy Siekkinen,[†] Addie Warsen,[‡] Zhi-Yuan Li,[§] Hui Zhang,[||] Younan Xia,*[,†] and Xingde Li*[,‡]

Department of Chemistry, Department of Bioengineering, University of Washington, Seattle, Washington 98195, Institute of Physics, Chinese Academy of Sciences, Beijing 10080, China, and Department of Pathology, Johns Hopkins University, Baltimore, MD 21231

Received February 12, 2007; Revised Manuscript Received April 2, 2007

ABSTRACT

Gold nanocages with a relatively small size (e.g., ∼45 nm in edge length) have been developed, and the structure of these nanocages was tailored to achieve strong absorption in the near-infrared (NIR) region for photothermal cancer treatment. Numerical calculations show that the nanocage has a large absorption cross section of 3.48×10^{-14} m^2, facilitating conversion of NIR irradiation into heat. The gold nanocages were conjugated with monoclonal antibodies (anti-HER2) to target epidermal growth factor receptors (EGFR) that are overexpressed on the surface of breast cancer cells (SK-BR-3). Our preliminary photothermal results show that the nanocages strongly absorb light in the NIR region with an intensity threshold of 1.5 W/cm^2 to induce thermal destruction to the cancer cells. In the intensity range of 1.5–4.7 W/cm^2, the circular area of damaged cells increased linearly with the irradiation power density. These results suggest that this new class of bioconjugated gold nanostructures, immuno gold nanocages, can potentially serve as an effective photothermal therapeutic agent for cancer treatment.

Gold nanostructures have attracted growing interest in biomedical research due to their unique optical and chemical properties in addition to their excellent biocompatibility.[1] The strong optical absorption of gold nanostructures suggests their great potential as a photothermal therapeutic agent.[2] Photothermal therapy is less invasive compared to chemotherapy or surgery and has drawn increased attention in cancer treatment. In photothermal therapy, optical irradiation is absorbed and transformed into heat, inducing thermal denaturing of proteins (and DNAs) in the cell and coagulation of tissue and, consequently, causing irreversible damage to the targeted tissue.[3] The use of gold nanostructures significantly enhances the absorption of light at specific wavelengths for heat conversion. In addition, convenient bioconjugation of gold nanostructures improves target selectivity, which therefore greatly reduces the required laser power for photothermal destruction of the targeted tissue and minimizes the collateral damage to surrounding healthy tissues. Studies have shown that gold nanoparticles conjugated with antibodies or viral vectors could effectively damage the targeted cancerous tissue when illuminated by light with wavelengths around the absorption peak of the gold nanoparticles.[4] One challenge is that gold nanoparticles (in particular, spherical ones) mainly absorb light in the visible range, which has a shallow penetration depth in tissue as compared to the therapeutic window in the near-infrared (NIR) region where blood and soft tissue are relatively transparent. Zharov and co-workers have demonstrated that aggregates of gold nanoparticles increased the photothermal effect in the NIR region.[5] These aggregates were formed during storage or by self-assembly on cell surface. In practice, the aggregate size and, consequently, the peak absorption wavelength are both very difficult to control. Over the past few years, many research efforts have been focused on developing novel gold nanostructures to achieve surface plasma resonance (SPR) in the NIR region. Halas and co-workers have developed 10 nm thick gold nanoshells supported on 110 nm diameter silica cores with a NIR absorption peak and demonstrated their use in photothermal ablation of cancer cells and tissue.[6] Recently, El-Sayed and co-workers have demonstrated that gold nanorods of 20 nm in diameter and 78 nm in length

* Corresponding authors. E-mails: xingde@u.washington.edu (X.L.); xia@chem.washington.edu (Y.X.).
[†] Department of Chemistry, University of Washington.
[‡] Department of Bioengineering, University of Washington.
[§] Institute of Physics, Chinese Academy of Sciences.
[||] Department of Pathology, Johns Hopkins University.

10.1021/nl070345g CCC: $37.00
Published on Web 04/13/2007

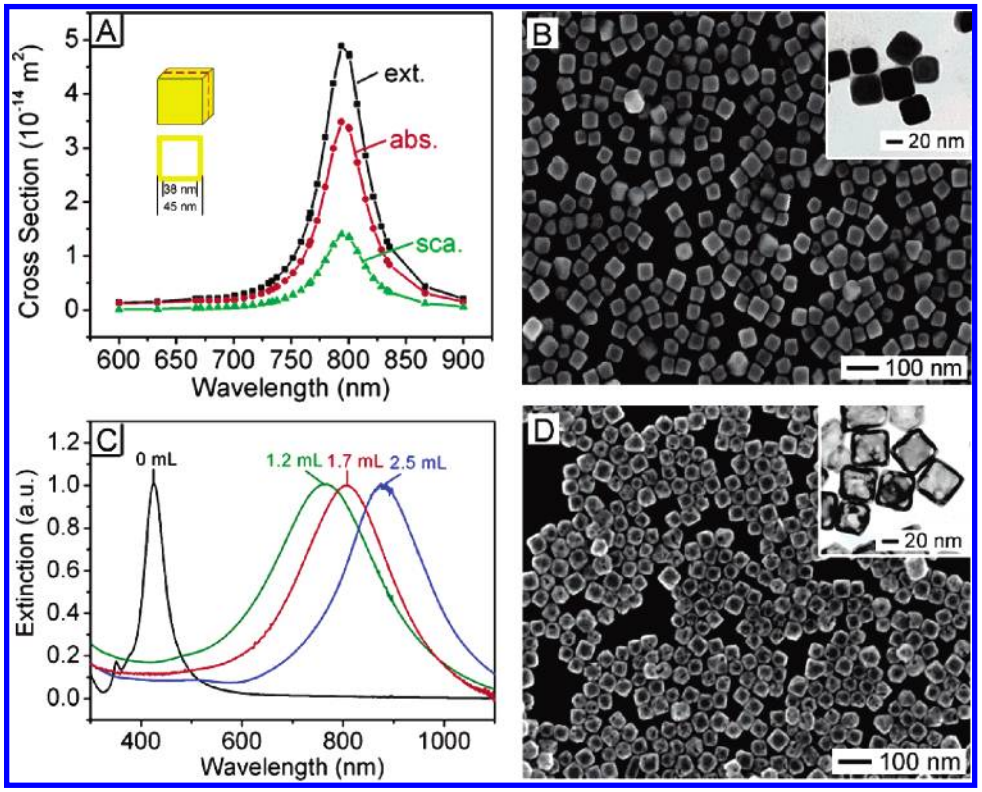

Figure 1. (A) Extinction (C_{ext}), absorption (C_{abs}), and scattering (C_{sca}) cross sections (note that $C_{ext} = C_{abs} + C_{sca}$) calculated using the DDA method for a gold nanocage of 45 nm in edge length and 3.5 nm in wall thickness, and with the geometry depicted in the inset in (D). The alloy composition of the nanocages is Au_3Ag. (B) SEM images of Ag nanocubes prepared by sulfide-mediated polyol synthesis. The inset shows TEM image of the Ag nanocubes. (C) Normalized Vis−NIR extinction spectra recorded from aqueous suspensions of nanostructures after titrating Ag nanocubes with different amounts of a $HAuCl_4$ aqueous solution. Note that the spectrum in red is corresponding to the Au nanocages shown in (D). (D) SEM image of Au nanocages prepared by refluxing an aqueous solution containing both silver nanocubes and $HAuCl_4$. The inset shows a TEM image of the Au nanocages.

have a longitudinal absorption mode in the NIR region and can also serve as a photothermal therapeutic agent.[7] However, it remains a grand challenge to develop gold nanostructures with all the dimensions smaller than 50 nm (i.e., much smaller than gold nanoshells) to potentially facilitate targeted delivery while retaining a strong NIR absorption and with easy-to-control synthesis conditions (e.g., without the need for a large amount of surfactant as required in gold nanorod synthesis). In this paper, we report a new class of potential photothermal therapeutic agents based on gold nanocages which have a size less than 50 nm and a strong resonance absorption peak tunable in the NIR region to precisely match the laser source with a central wavelength around 810 nm. The synthesis of gold nanocages can be conveniently controlled with a superb repeatability. In vitro studies have demonstrated that the gold nanocages conjugated with cancer cell specific antibodies are very effective for photothermal destruction of cancer cells with a much lower laser irradiation threshold than previously reported for other gold nanostructures.

Gold nanocages are a class of recently developed nanostructures having a hollow interior and a thin, porous but robust wall.[9] To synthesize gold nanocages with a strong SPR absorption around 810 nm (i.e., the central wavelength of the laser used in the later photothermal studies), numerical calculations based on discrete dipole approximation (DDA) were carried out.[10] Figure 1A shows that a gold nanocage of 45 nm in edge length and 3.5 nm in wall thickness (and with 25% residual silver alloyed with gold) can provide an absorption-dominant SPR peak around 810 nm. The C_{abs} and C_{sca} were found to be 3.48×10^{-14} m^2 and 1.41×10^{-14} m^2, respectively, with a C_{abs}/C_{sca} ratio of ~2.5. Although smaller nanocages (e.g., 35 nm in edge length) may have an even higher C_{abs}/C_{sca} ratio, the absolute value of C_{abs} decreases by a factor of ~5 when the edge length changes from 45 to 35 nm. As a compromise, we chose to use the 45 nm nanocages for our initial photothermal study, which have a large absorption cross section while still maintaining a relatively compact size.

Gold nanocages with the targeted edge length of 45 nm were then synthesized using galvanic replacement reaction between silver nanocubes (of ~40 nm in edge length, serving as sacrificial templates) and chloroauric acid. Figure 1B shows SEM and TEM images of Ag nanocubes that were synthesized using a recently reported sulfide-mediated polyol process that is well-suited for mass production.[8] Figure 1C shows the normalized extinction spectra of the gold nanocages, the peaks of which vary with the molar ratio of Ag nanocubes to chloroauric acid, resulting in different void sizes in the interior, wall thicknesses, and pore sizes on the wall. By simply controlling this molar ratio, the extinction peak of gold nanocages can be conveniently tuned over a broad spectral range spanning from the visible to the NIR. Figure 1D shows the SEM and TEM images of the as-synthesized

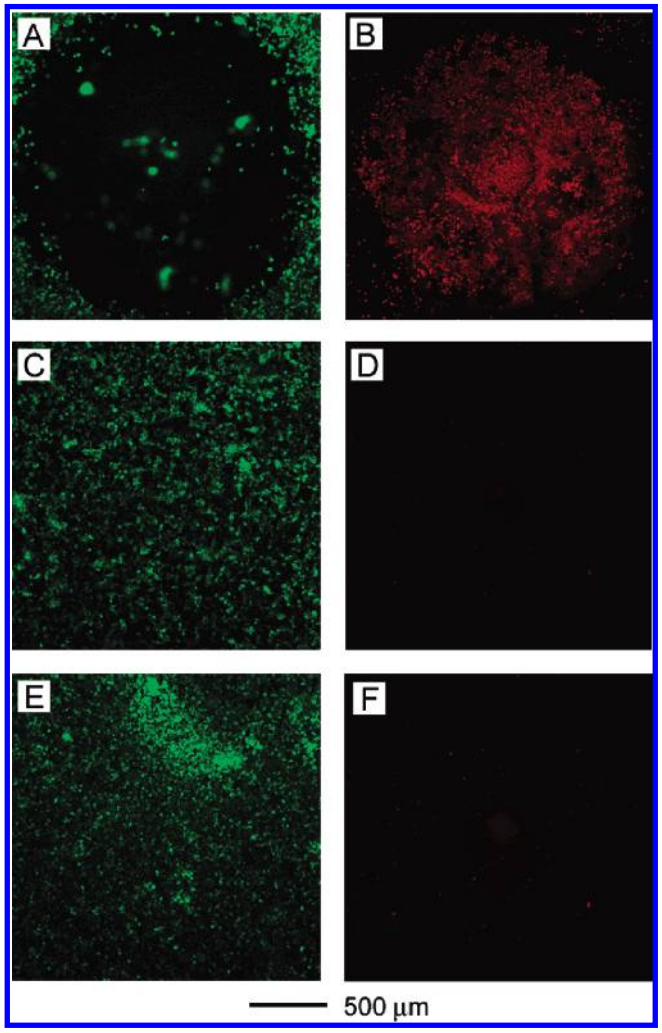

Figure 2. SK-BR-3 breast cancer cells that were treated with immuno gold nanocages and then irradiated by an 810 nm laser at a power density of 1.5 W/cm^2 for 5 min showed a well-defined circular zone of dead cells as revealed by: (A) calcein AM assay (where green fluorescence indicates the cells were live), and (B) ethidium homodimer-1 (EthD-1) assay (where red fluorescence indicates the cells were dead). In the control experiment, cells irradiated under the same conditions but without immuno gold nanocage treatment maintained viability, as indicated by (C) calcein fluorescence assay and (D) the lack of intracellular EthD-1 uptake. Cells treated with immuno gold nanocages but irradiated at a lower power density (0.5 W/cm^2) for 5 min remained alive, as shown by (E) calcein fluorescence assay and (F) the lack of intracellular EthD-1 uptake.

gold nanocages with their extinction peak tuned to 810 nm. As detailed elsewhere,[9] each nanocage has the corners truncated in addition to possible small openings on each facet. The measured edge length and wall thickness of these nanocages are 45 ± 4 and 3.5 ± 0.5 nm, respectively, which were averaged from 50 nanocages based on their TEM images. These results were close to the values estimated from the stoichiometry for the galvanic replacement reaction (i.e., oxidation of every three Ag atoms generates one Au atom). From both the EDX and AES analysis, these nanocages were composed of 75% Au and 25% Ag in a state of alloy. The experimentally measured SPR peak position is consistent with the result predicted by DDA calculation. The discrepancy in the peak width could be attributed to the small but non-negligible variations in the nanocage size, wall thickness, and the degree of corner truncation. On the basis of our recent calculations,[10] the peak position is not sensitive to the number and size of pores on the wall of a gold nanocage.

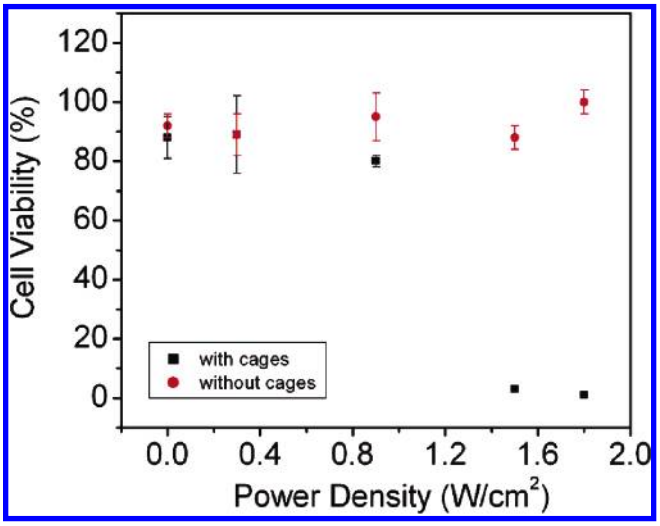

Figure 3. Cell viability study as represented by the calcein live-cell green fluorescence (normalized by the calcein fluorescence from a nonirradiated cell sample) versus the power density of NIR laser; (■) cells incubated with immuno gold nanocages and (●) cells without immuno gold nanocage treatment.

A well-characterized breast cancer cell line, SK-BR-3, which overexpresses the epithermal growth factor receptor 2 (EGFR2 or HER2) on the cell surface, has been used to demonstrate the photothermal effect of the gold nanocages. For active targeting, the gold nanocages were bioconjugated following the previously reported two-step procedure.[9,10] In essence, we first functionalized the nanocages with thiolated polyethylene glycol (PEG) and then conjugated the PEGylated nanocages with monoclonal anti-HER2 antibodies to selectively target the antigens (EGFR2) on the SK-BR-3 cell surface. After conjugation, we noticed that the SPR peak of the nanocages slightly red-shifted to 812 nm, which was expected due to the change in refractive index around the surface of gold nanocages. The immuno gold nanocages remain well-dispersed with a stable SPR spectrum in saline and can be stocked for a couple of weeks.

Using the immuno gold nanocages, we have demonstrated selective photothermal destruction of cancer cells in vitro. The NIR irradiation source was a home-built Kerr-lens mode-locked Ti:sapphire laser with a 82 MHz repetition rate. The laser spectrum centered at 810 nm with a bandwidth of 120 nm. The laser beam was delivered to the target through a 5 m long single-mode fiber (SMF), followed by a convex lens. The temporal pulse width was broadened to ~20 ps after the SMF fiber. The beam focus was about 150 mm away from the lens, and the measured focused spot size was about 70 μm. The beam spot size after the focused spot can be accurately predicted by Gaussian beam optics. We chose to place the sample (cell culture) about 140 mm away from the beam focus, and the corresponding irradiation spot size at the sample was about 2 mm in diameter, given by Gaussian optics. The irradiation spot size on cell culture was

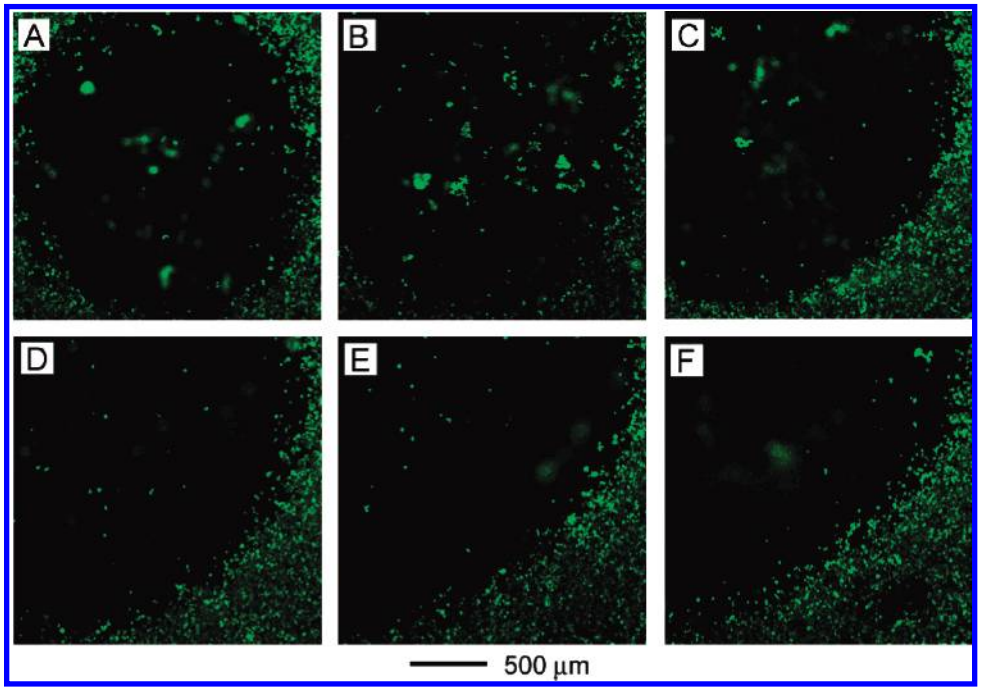

Figure 4. Cells that were first incubated with immuno gold nanocages and then irradiated by NIR laser for 5 min at different power densities: (A) 1.5, (B) 2.0, (C) 2.5, (D) 3.0, (E) 3.5, and (F) 4.7 W/cm^2. As revealed by the calcein AM assay, the green florescence images clearly show the size of the damaged area which lacks green fluorescence increases with the irradiation power density.

fixed to 2 mm in diameter for all the samples and at all irradiation powers. The laser power was adjusted by a variable neutral density filter and measured using a calibrated power meter (Newport Co., model 840). Cancer cells (10^6 cells per mL) were reseeded on a 24-well plate. When the confluence reached about 100%, the cells in different wells were treated with the same but excessive amount of immuno gold nanocages. The use of excessive gold nanocages was to saturate the specific binding sites on the cell surface and achieve a similar density of nanocages per well.

To find the threshold NIR irradiation power density for inducing photothermal destruction to cancer cells that were targeted with immuno gold nanocages, various laser power densities were used with a fixed irradiation area of 2 mm in diameter and irradiation duration of 5 min. The samples were incubated with calcein AM and ethidium homodimer 1 (EthD-1) following the standard staining protocols and then examined by fluorescence microscopy. The colorless calcein AM will be enzymatically converted to green fluorescence calcein only in viable cells, while EthD-1 can penetrate through cells, stain DNAs, and emit red fluorescence only when the cell membrane is irreversibly compromised (e.g., by photothermal damage as in this study). Our studies indicate that, when the laser power density reached 1.5 W/cm^2, cancer cells in all samples treated with immuno gold nanocages exhibited loss of viability within the laser irradiation spot, as determined by calcein AM (for live cells) and EthD-1 (for dead cells) staining assay. As shown in Figure 2A, the circular NIR irradiated region shows basically no green calcein fluorescence, indicating the loss of live cells due to photothermal destruction. The EthD-1 staining image of the same sample is shown in Figure 2B, and the red fluorescence region corresponds nicely to the void region in the green calcein fluorescence image (Figure 2A), reconfirming cell death over the same region that was irradiated. Furthermore, the diameter of the circular region matches the laser spot size (i.e., 2 mm), confirming that cell death was caused by and confined to the NIR irradiation. In control experiments, cancer cells that were only incubated with cell culture medium exhibited no loss of viability after NIR irradiation under the same conditions, as shown in Figures 2C (calcein AM staining) and 2D (EthD-1 staining), respectively. It is noticed that, when the laser irradiation power density was less than 1.5 W/cm^2, the fluorescence images from the cell samples that were treated with immuno gold nanocages appear similar to the control cell fluorescence images (see Figures 2E and 2F), suggesting a NIR irradiation threshold around 1.5 W/cm^2 for inducing photothermal damage.

To quantify the cancer cell viability versus NIR irradiation power, the irradiated cells were stained with calcein AM right after irradiation, and the green fluorescence was measured using a microplate reader. At each irradiation power, three wells of cancer cells with ~100% confluence were first incubated with immuno gold nanocages, followed by PBS washing and then NIR irradiation. Three control cell wells that were not incubated with immuno nanocages were also irradiated by the same NIR power under the same illumination condition. The green fluorescence light intensity from the three nanocage-treated cell wells and the three control wells was respectively averaged and then normalized by the calcein fluorescence from a sample that was not irradiated by NIR laser nor treated with immuno nanocages. The cell viability was then represented by the normalized calcein fluorescence signal. Figure 3 illustrates the cell viability versus irradiation power density for both cells with and

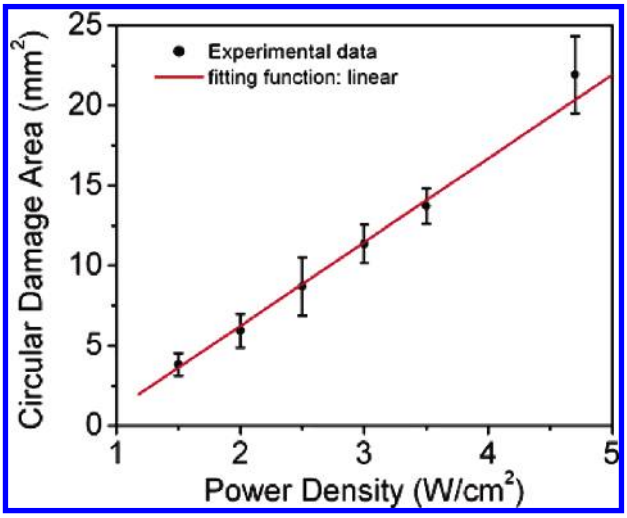

Figure 5. Plot of the circular cell destruction area against irradiation power density. The experimentally measured photothermal damage area was roughly linear with respect to the irradiation power density as indicated by the red line.

without treatment by immuno nanocages. We find the transition power range for inducing damage is between 0.9 and 1.5 W/cm^2. The cell viability exhibits significant decrease at an irradiation power density of ~1.5 W/cm^2, which is consistent with the previous qualitative observation. We also notice that the fluorescence light intensity from all control cell wells remains nearly unchanged in spite of the different irradiation power.

Interestingly, we also found that the circular area of cell damage increased with irradiation power density in the presence of immuno gold nanocages. Figure 4 shows the fluorescence images of immuno nanocage-targeted cancer cells stained with calcein AM after NIR irradiation with different power densities but the same irradiation beam spot size. We found that the region of photothermal cell damage increased with the power density and went beyond the irradiation beam spot size on the cell sample. This is expected because the heat harvested from NIR irradiation would increase as the power density increased and transfer to regions beyond the irradiation beam spot size. Figure 5 shows a plot of the circular cell damage area as a function of irradiation power density, which roughly follows a linear relationship. The detail relationship can be rather complex, depending on the heat conduction efficiency of the medium, the finite sample size, and the sample boundaries conditions, which is beyond the scope of this report.

In summary, 45 nm gold nanocages were successfully synthesized and their SPR peaks were precisely tuned to 810 nm to match the center wavelength of laser irradiation for photothermal cancer treatment. The nanocages were conveniently functionalized with thiolated PEG and then conjugated with HER2-antibody to target EGFR2 that are overexpressed on the surface of SK-BR-3 breast cancer cells. Our preliminary photothermal studies with the immuno gold nanocages show that they strongly absorb at their SPR peak wavelength, with a photothermal cell damage power density threshold of ~1.5 W/cm^2. This threshold for selective destruction of cancer cells is substantially lower than those reported for gold nanoshells (35 W/cm^2)[6c] and gold nanorods (10 W/cm^2).[7] This lower thermal damage threshold is unlikely caused by the formation of microbubbles when using a femtosecond laser because the 1.5 W/cm^2 threshold corresponds to an irradiation energy density per pulse of only about 18 nJ/cm^2, which was far below the threshold (~0.6 J/cm^2) for microbubble formation.[11] Thus the large absorption cross section of the gold nanocages might be the key factor contributing to the reduction of the thermal damage threshold (in conjunction with other parameters such as the density of nanocages on each cell). In control experiments, cells without derivatization by immuno gold nanocages exhibited no observable loss of viability under the same experimental conditions. These results suggest that immuno gold nanocages with a size less than 50 nm are a promising new class of photothermal therapeutic agents for cancer treatment.

Acknowledgment. This work was supported in part by NIH (1R01 CA120480, X.L.), an NSF CAREER Award (X.L.), NSF (DMR-0451788, Y.X.), and a Camille Dreyfus Teacher Scholar Award (Y.X.). Y.X. is supported in part by the NIH Director's Pioneer Award (5DP1OD000798). Z.Y.L. was supported by the National Key Basic Research Special Foundation of China (No. 2004 CB719804). L.A. thanks the Center for Nanotechnology at the University of Washington for an IGERT Fellowship Award supported by NSF. Both SEM and EDX studies were performed at the Nanotech User Facility (NTUF), a member of the National Nanotechnology Infrastructure Network (NNIN) funded by NSF.

References

(1) (a) Hu, M.; Chen, J.; Li, Z.-Y.; Au, L.; Hartland, G. V.; Li, X.; Marquez, M.; Xia, Y. *Chem. Soc. Rev.* **2006**, *35*, 1084. (b) Xia, Y.; Halas, N. J. *MRS Bull.* **2005**, *30*, 338.

(2) Pissuwan, D.; Valenzuela, S. M.; Cortie, M. B. *Trends Biotechnol.* **2006**, *24*, 62.

(3) Anderson, R. R.; Parrish, J. A. *Science* **1983**, *220*, 524.

(4) (a) Everts, M.; Saini, V.; Leddon, J. L.; Kok, R. J.; Stoff-Khalili, M.; Preuss, M. A.; Millican, L. C.; Perkins, G.; Brown, J. M.; Bagaria, H.; Nikles, D. E.; Johnson, D. T.; Zharov, V. P.; Curiel, D. T. *Nano Lett.* **2006**, *6*, 587. (b) El-Sayed, I. H.; Huang, X.; El-Sayed, M. A. *Cancer Lett.* **2006**, *239*, 129. (c) Huang, X.; Jain, P. K.; El-Sayed, I. H.; El-Sayed, M. A. *Photochem. Photobiol.* **2006**, *82*, 412. (d) Pitsillides, C. M.; Joe, E. K.; Wei, X.; Anderson, R. R.; Lin, C. P. *Biophys. J.* **2003**, *84*, 4023. (e) Zharov, V.; Galitovsky, V.; Viegas, M. *Appl. Phys. Lett.* **2003**, *83*, 4897.

(5) (a) Khlebtsov, B.; Zharov, V.; Melnikov, A.; Tuchin, V.; Khlebtsov, N. *Nanotechnology* **2006**, *17*, 5167. (b) Zharov, V. P.; Letfullin, R. R.; Galitovskaya, E. *J. Phys. D: Appl. Phys.* **2005**, *38*, 2571. (c) Zharov, V. P.; Letfullin, R. R.; Galitovskaya, E. *Laser Surg. Med.* **2005**, *37*, 219.

(6) (a) Loo, C.; Lowery, A.; Halas, N.; West, J.; Drezek, R. *Nano Lett.* **2005**, *5*, 709. (b) O'Neal, D. P.; Hirsch, L. R.; Halas, N. J.; Payne, J. D.; West, J. L. *Cancer Lett.* **2004**, *209*, 171. (c) Hirsch, L. R.; Stafford, R. J.; Bankson, J. A.; Sershen, S. R.; Rivera, B.; Price, R. E.; Hazle, J. D.; Halas, N. J.; West, J. L. *Proc. Natl. Acad. Sci. U.S.A.* **2003**, *23*, 13549.

(7) Huang, X.; El-Sayed, I. H.; Qian, W.; El-Sayed, M. A. *J. Am. Chem. Soc.* **2006**, *128*, 2115.

(8) Siekkinen, A. R.; McLellan, J. M.; Chen, J.; Xia, Y. *Chem. Phys. Lett.* **2006**, *432*, 491.

(9) Chen, J.; Saeki, F.; Wiley, B.; Cang, H.; Cobb, M. J.; Li, Z.-Y.; Au, L.; Zhang, H.; Kimmey, M. B.; Li, X.; Xia, Y. *Nano Lett.* **2005**, *5*, 473.

(10) Chen, J.; Wiley, B.; Li, Z.; Cang, H.; Campbell, D.; Saeki, F.; Au, L.; Lee, J.; Li, X.; Xia, Y. *Adv. Mater.* **2005**, *17*, 2255.

(11) Lapotko, D. O.; Lukianova, E.; Oraevsky, A. A. *Laser Surg. Med.* **2006**, *38*, 631.

NL070345G